Engineering Specificity for Folate into Dihydrofolate Reductase from *Escherichia coli*†

Bruce A. Posner,‡ Luyuan Li,§ Richard Bethell,|| Tomoko Tsuji,⊥ and Stephen J. Benkovic*,#

Pharmacology Department, University of Texas Southwest Medical Center, 5323 Harry Hines Boulevard, Dallas, Texas 75235-9401, Medical Research Division, American Cyanamid Company, Pearl River, New York 10965, Department of Virology, Glaxo Group Research Limited, Greensford Road, Middlesex, UB6 0HE, U.K., Sagami Chemical Research Center, 4-4-1 Nishi-Ohnuma Sagamihara, Kanagawa 229, Japan, and Chemistry Department, Pennsylvania State University, 152 Davey Laboratory, University Park, Pennsylvania 16802

Received August 3, 1995; Revised Manuscript Received November 2, 1995⊗

ABSTRACT: Despite several similarities in structure and kinetic behavior, the bacterial and vertebrate forms of the enzyme dihydrofolate reductase (DHFR) exhibit differential specificity for folate. In particular, avian DHFR is 400 times more specific for folate than the *Escherichia coli* reductase. We proposed to enhance the specificity of the *E. coli* reductase for folate by incorporating discrete elements of vertebrate secondary structure. Two vertebrate loop mutants, VLI and VLII containing 3−7 additional amino acid insertions, were constructed and characterized by using steady-state kinetics, spectrofluorimetric determination of ligand equilibrium dissociation constants, and circular dichroism spectroscopy. Remarkably, the VLI and VLII mutants are kinetically similar to wild-type *E. coli* reductase when dihydrofolate is the substrate, although VLII exhibits prolonged kinetic hysteresis. Moreover, the VLI dihydrofolate reductase is the first mutant form of *E. coli* DHFR to display enhanced specificity for folate [$(k_{cat}/K_m)_{mutant}/(k_{cat}/K_m)_{wt} = 13$]. A glycine−alanine loop (GAL) mutant was also constructed to test the design principles for the VLI mutant. In this mutant of the VLI reductase, all of the residues from positions 50 to 60, except the strictly conserved amino acids Leu-57 and Arg-60, were converted to either glycine or alanine. A detailed kinetic comparison of the GAL and wild-type reductases revealed that the mutations weaken the binding by both cofactor and substrate by up to 20-fold, but under saturating conditions the enzyme exhibits a k_{cat} value nearly identical to that of the wild type. The rate of hydride transfer is reduced by a factor of 30, with a compensating increase in the dissociation rate for tetrahydrofolate. Although key stabilizing interactions have been sacrificed (it shows no activity toward folate), the maintenance of the correct register between key residues preserves the activity of the enzyme toward its natural substrate. Collectively, neither specific proximal point site mutations nor larger, more distal secondary structural substitutions are sufficient to confer a specificity for folate reduction that matches that observed with the avian enzyme. This is consistent with the hypothesis that the entire protein structure must contribute extensively to the enzyme's specificity.

Redesign of enzyme architecture has proven to be a useful means of generating novel biological catalysts (Johnson & Benkovic, 1990; Dunn et al., 1991; Fersht & Winter, 1992). This approach assumes that the architecture of an extensively characterized enzyme is a starting point for designing a new catalyst. Many early efforts attempted to alter substrate specificity with only a few changes in active site composition (Johnson & Benkovic, 1990; Fersht & Winter, 1992). The results of these experiments suggested that many alterations are necessary at sites proximal and distal to the site of chemical transformation. Recent studies with lactate dehydrogenase from *Bacillus stearothermophilus* and with trypsin from rat demonstrate the extent to which an enzyme's architecture must be altered to optimize specificity for a new substrate (Dunn et al., 1991; Hedstrom et al., 1992; Wilks et al., 1992). With similar design principles in mind, we have sought to define the structural features responsible for differential substrate specificities exhibited by bacterial and vertebrate forms of dihydrofolate reductase.

Dihydrofolate reductase (DHFR)[1,2] catalyzes the reduction of 7,8-dihydrofolate (H_2F) to 5,6,7,8-tetrahydrofolate (H_4F)

† This work was supported by PHS Grant No. GM24129.
‡ University of Texas Southwest Medical Center.
§ American Cyanamid Company.
|| Glaxo Group Research Limited.
⊥ Sagami Chemical Research Center.
Pennsylvania State University.
⊗ Abstract published in *Advance ACS Abstracts,* January 15, 1996.

[1] Abbreviations: DHFR, dihydrofolate reductase; H_2F, dihydrofolate; H_4F, tetrahydrofolate, NH or NADPH, nicotinamide adenine dinucleotide phosphate, reduced; $NADP^+$ or N^+, nicotinamide adenine dinucleotide phosphate; MTX, methotrexate; DAM, 2,4-diamino-6,7-dimethylpteridine; VLI, vertebrate loop I; VLII, vertebrate loop II; GAL, glycine−alanine loop; CD, circular dichroism; L54G, leucine 54 in *E. coli* dihydrofolate reductase mutated to glycine; L54N, leucine 54 in *E. coli* dihydrofolate reductase mutated to asparagine; D27E, aspartate 27 in *E. coli* dihydrofolate reductase mutated to glutamate; L28F, leucine 28 in *E. coli* dihydrofolate reductase mutated to phenylalanine.

[2] The pK_a of the E−NH complex can be determined by competitive inhibition or fluorescence binding studies with 2,4-diamino-6,7-dimethylpteridine (DAM; Cleland, 1977; Stone & Morrison, 1983; Taira & Benkovic, 1988). Protonation of the inhibitor causes a quenching of inhibitor fluorescence. However, in certain fluorescence binding experiments with DAM, inhibitor fluorescence did not decrease with the addition of enzyme. This observation suggests that DAM is not protonated upon binding to VLI DHFR (Taira & Benkovic, 1988). Therefore, inhibition studies would not necessarily yield the pK_a of Asp-27 in the E−NADPH complex.

0006-2960/96/0435-1653$12.00/0

by transferring the *pro-R*-hydrogen of NADPH to C6 of the pterin substrate (Blakley, 1985). DHFR will also catalyze the reduction of folate to H_4F, albeit less efficiently than the reduction of dihydrofolate. Interestingly, specificity for folate (k_{cat}/K_m) is higher for vertebrate forms of the enzyme than bacterial DHFRs. For example, under identical conditions of ionic strength and pH, chicken DHFR is approximately 400 times more specific for folate than the *Escherichia coli* form of the enzyme.

We sought to enhance the specificity of the *E. coli* reductase for folate by incorporating discrete elements of vertebrate secondary structure. In designing and characterizing the mutant bacterial reductases, we have relied heavily on previous characterizations of both wild-type and mutant DHFRs, as well as on statistical and structural classifications of secondary structure. Three mutant DHFRs, vertebrate loop I (VLI), vertebrate loop II (VLII), and a glycine−alanine loop (GAL), were constructed and characterized by using published methodologies [Fierke et al. (1987) and references therein]. While all mutant reductases retained remarkable catalytic activity toward H_2F, only VLI DHFR exhibited a 13-fold increase in the rate of reduction of folate. The analysis of pre- and steady-state kinetic data along with thermodynamic measurements of ligand binding, however, provided key insights into the nature and extent of global interactions within the protein that are allied with its enzymic activity.

MATERIALS AND METHODS

Escherichia coli Strains, Biochemical Reagents, and DNA Manipulations. *E. coli* strains were maintained and manipulated as described previously (Wagner et al., 1992). All oligonucleotides were synthesized and purified by the Penn State Biotechnology Facility. Manipulations and analyses of recombinant DNA were carried out by using standard protocols (Sambrook et al., 1989).

Substrates, Inhibitors, and Buffers. The substrates for DHFR were prepared by using published methods (Blakley, 1960; Fierke et al., 1987; Andrews et al., 1989). NADPH and NADP were purchased from Sigma. 5,6(*S*),7,8-Tetrahydrofolate (H_4F) was prepared by enzymatic reduction of H_2F with *E. coli* DHFR and purified as previously described (Curthoys et al., 1972). Concentrations of substrates and inhibitors were determined spectrophotometrically by using published extinction coefficients [see Fierke et al. (1987) and references therein]. [4′(*R*)-^{2}H]NADPH (NADPD) was prepared by using alcohol dehydrogenase from *Leuconostoc mesenteroides* as described by Viola and co-workers (Viola et al., 1979).

Construction of Mutant E. coli DHFRs. Mutant genes were constructed by using a combination of oligonucleotide-directed and cassette mutagenesis (Li & Benkovic, 1991; Wagner et al., 1992). Specific details of their construction are available upon request. Complete sequence analysis was performed on each mutant gene.

Enzyme Purification. With the exception of the VLII mutant, mutant and wild-type *E. coli* DHFRs were purified essentially as described by Baccanari and co-workers (Baccanari et al., 1977). After elution from the MTX affinity column, the VLII mutant was purified to homogeneity on a DEAE Sephacel column, using a stepwise gradient with KCl. The mutant protein eluted at a salt concentration of 0.2 M.

Chicken liver dihydrofolate reductase was purified as previously described (Kaufman & Kemerer, 1977; Stone & Morrison, 1986). One kilogram of livers routinely yielded 4−6 mg of DHFR with a specific activity of 13−13.5 units/mg (Kaufman & Kemerer, 1977).

All protein preparations were shown to be homogeneous and free of contaminating ligands by SDS−polyacrylamide gel electrophoresis and UV−visible absorbance spectroscopy, respectively. Protein concentrations were determined by active site titration with methotrexate (MTX).

Steady-State Kinetics. Kinetic assays were conducted in MTEN buffer [50 mM 2-morpholinoethanesulfonic acid (MES), 25 mM tris(hydroxymethyl)aminomethane (Tris), 25 mM ethanolamine, and 100 mM sodium chloride, pH 5.0−10.0] at 25 °C. Initial velocity studies for dihydrofolate and folate reduction were carried out by using a Cary 219 UV−visible spectrophotometer at 340 nm. Mutant and wild-type DHFRs were preincubated with NADPH for 2−5 min prior to initiation of the reaction with H_2F or folate to eliminate hysteretic behavior (Penner & Frieden, 1985). Preincubation periods of 20−30 min were required with VLII DHFR to completely eliminate hysteretic behavior. Initial rates were calculated by using a molar absorbance change of 11 800 M^{-1} cm^{-1} (Stone & Morrison, 1982).

Michaelis parameters (k_{cat} and K_m) were determined at several pH's by varying either NADPH or H_2F. Data were analyzed according to eq 1 by using the nonlinear least-squares regression program RS1 on a Vax microcomputer.

$$v = \frac{k_{cat}S}{K_m + S} \tag{1}$$

$$y = \frac{C[H]}{K_a + [H]} \tag{2}$$

pH-independent values for k_{cat} and K_m were determined along with standard errors by using eq 2, where C is the pH-independent value of the kinetic parameter, K_a is the acid dissociation constant, and [H] is the proton concentration at a particular pH. Unless explicitly noted, this equation was used to fit all pH-dependent data.

Transient Kinetics. Transient binding and pre-steady-state kinetic studies were conducted on a stopped-flow spectrophotometer (Applied Photophysics, Inc.) with a 1.4-ms dead time (Wagner et al., 1992). After mixing, fluorescence and absorbance data were collected over a selected time interval (20 ms to 5 min) and stored on an Archimedes personal computer. Data were fit to a single-exponential model, a single-exponential model followed by a linear rate, or a double-exponential model by nonlinear least-squares regression with a computer program supplied by the instrument manufacturer. Kinetic data were then transferred to a Vax microcomputer for further analysis using the program KINSIM (Barshop et al., 1983).

Equilibrium Dissociation Constants. Excitation of *E. coli* and avian reductases at 290 nm is accompanied by fluorescence emission at 340 and 325 nm, respectively. Thermodynamic dissociation constants (K_d's) were measured by following the quenching of intrinsic enzyme fluorescence upon the addition of ligand at 25 °C in MTEN buffer. All additions were allowed to reach equilibrium before the fluorescence intensity was recorded (2−7 min). As a control

experiment, a known concentration of tryptophan was titrated in parallel with the enzyme sample to correct for inner filter effects due to absorbance of the added ligand. Measurements were made by using an SLM8000 spectrofluorimeter (SLM-Aminco Inc.).

Data were fit to the following equation:

$$F = \frac{F_E - C(F_E - F_{EL})}{2[E_T]} \quad (3)$$

where

$$C = [E_T] + [L_T] + K_d - [([E_T] + [L_T] + K_d)^2 - 4\,[E_T][L_T]]^{1/2}$$

F_E and F_{EL} are the initial and final fluorescence measurements, respectively (Taira et al., 1987). $[E_T]$ and $[L_T]$ are the total enzyme and ligand concentrations, respectively. Acceptable determinations of dissociation constants were made by using enzyme concentrations equal to or slightly less than the K_d.

Circular Dichroism Spectra. Circular dichroism spectra were collected by using a AVIV 62DS spectropolarimeter at 25 °C in 10 mM phosphate, 0.2 mM EDTA, and 1 mM β-mercaptoethanol (pH 7.8). Spectra were recorded from 180 to 350 nm using a 5-s averaging time and a 1-mm-path-length cell containing 0.5 mg of protein/mL of buffer. Data collected for protein samples were corrected by using spectra obtained in the absence of protein and expressed in terms of the mean residue ellipticity (MRE) using the following equation:

$$\mathrm{MRE} = \frac{100(\mathrm{MW})}{(\mathrm{PL})(\mathrm{PC})(\mathrm{NR})} \quad (4)$$

where MW is the protein molecular weight, PL is the cell path length in centimeters, PC is the protein concentration in mg/mL, NR is the number of residues, and the factor of 100 derives from the conversion of the molar concentration to the decimole/(centimeter)^3 concentration unit (Schmid, 1990).

RESULTS

Design of VLI, VLII, and GAL E. coli DHFRs. The key to altering the specificity (k_{cat}/K_m) of the bacterial enzyme for folate is modifying the physical relationship between C4 of the pyridine ring and C7 of folate in the substrate ternary complex.[3] Theoretical and X-ray crystallographic studies suggest that enzyme-catalyzed reductions of the 5,6- and 7,8-double bonds proceed through *syn* and *anti* transition states, respectively (Wu & Houk, 1987, 1991; Bystroff et al., 1990; Davies et al., 1990). Reduction of both bonds requires a donor−acceptor distance of 2.6 Å. By using these criteria, Bystroff and co-workers constructed a hypothetical Michaelis complex (E−NH−H_2F) for *E. coli* DHFR that required reorienting enzyme residues and enforcing an upward pucker at C7 in the otherwise planar pteridine ring (Bystroff et al., 1990). By using folate binding data and their model for H_2F binding, these authors suggest that irrevocable misalignment

[3] After our work was completed, a revision of the structural model for catalysis was published (Reyes et al., 1995). We consider aspects of this new model in the Discussion section.

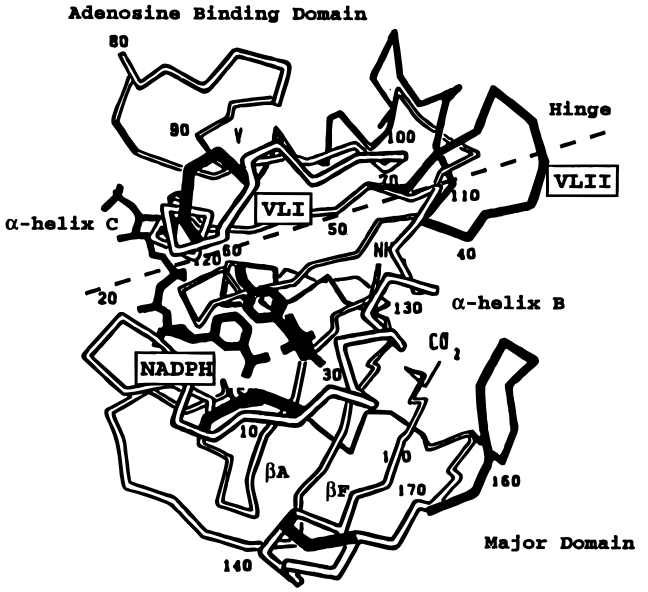

FIGURE 1: Superposition of *L. casei* and chicken DHFRs with the inhibitor 2,4-diamino-5,6-dihydro-6,6-dimethyl-5-(4′-methoxyphenyl)-*s*-triazine (Mϕ*T*) and NADPH bound (Volz et al., 1982). The filled-in backbone represents the chicken structure in regions where insertions and deletions occur. The superposition of the *E. coli* and chicken structures was nearly identical to that shown here. The domains are labeled as described by Bystroff and Kraut (1991).

```
Avian : -I60-P61-E62-K63-N64-R65-P66-L67-K68-D69-R70-I71-
E.coli: -I50-G51-----------R52-P53-L54-P55-G56-R57-K58-
VLI   : -I50-P51-E52-K53-N54-R55-P56-L57-K58-D59-R60-I61-
GAL   : -I50-G51-A52-G53-A54-G55-A56-L57-G58-A59-R60-K61-
     <-----]                                    [---->
  α-helix C                                    β-strand C

Avian : -T38-S39-T40-S41-H42-V43-E44-G45-K46-Q47-N48-A49-
E.coli: -T35-L36---------------------------N37-K38-P39-
VLII  : -T35-S36-T37-S38-H39-V40-E41-G42-K43-Q44-N45-A46-
      <-------------]                          [------->
    α-helix B                                  β-strand B
```

FIGURE 2: Alignment of wild-type and mutant sequences.

of the C7 of folate with the C4 of the coenzyme renders it a poor substrate. In contrast, the vertebrate enzyme appears to position both substrates in conformations that are optimal for hydride transfer (Davies et al., 1990), perhaps due to the slightly larger dimensions of its active site.

Despite a high degree of structural homology among vertebrate and bacterial reductases (Figure 1; Volz et al., 1982), vertebrate DHFRs contain additional residues in loops and turns that connect elements of secondary structure. In particular, vertebrate loop I (VLI) and vertebrate loop II (VLII) are larger than their bacterial counterparts, and each substructure could exert a significant influence on active site dimension (Figure 2). The VLI sequence is a vital part of the substrate binding site and serves to connect α-helix C to β-strand C, secondary structures that contribute to both the folate and coenzyme binding sites. This loop has previously been implicated as a major contributor to the larger dimensions of the active site in chicken DHFR, compared with the *E. coli* form of the enzyme, and may contribute to substrate specificity differences (Matthews et al., 1985). The VLII substructure occurs 15−20 Å from the active site and connects α-helix B and β-strand B. It is part of a "hinge" region that connects the adenosine binding domain (residues 38−88, *E. coli* numbering) and the major domain (residues 1−37 and 89−159, *E. coli* numbering; Bystroff & Kraut, 1991). Both domains contain multiple contacts with the

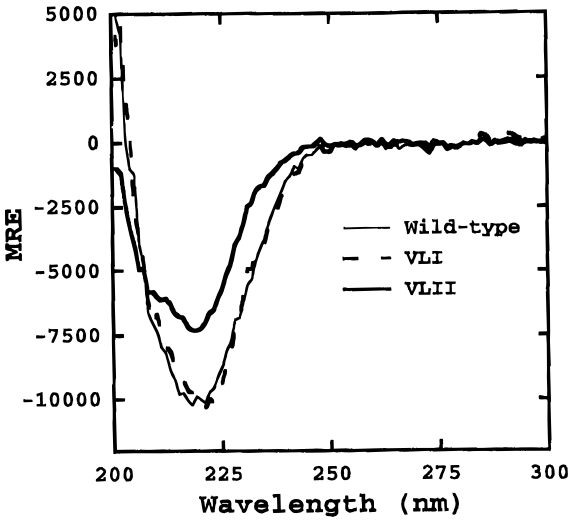

FIGURE 3: Circular dichroism of wild-type and mutant DHFRs. Each spectrum was collected as described in the Materials and Methods section (see text). The spectra shown are delineated as follows: wild-type *E. coli*, bold solid line; VLI, thin solid line; VLII, dashed line.

coenzyme and substrate. VLII may mediate important conformational changes that optimize the proximity of the reactants for hydride transfer, and its incorporation into the bacterial enzyme might also add flexibility to the active site.

A principal difficulty in designing the VLI and VLII mutants is deciding how much of the vertebrate structure to incorporate into the bacterial enzyme. Recent efforts to define the initiation and termination sequences of helices have emphasized the importance of preserving the hydrogen-bonding interactions between the helix and the secondary structure preceding and following it in the peptide chain (Presta & Rose, 1988; Richardson & Richardson, 1988; Harper & Rose, 1993). Although there is experimental support for these concerns [see Harper and Rose (1993) and references therein], it has also been demonstrated that helix boundaries can be "flexible" and dependent on ionic interactions with the helix dipole (Fairman et al., 1989; Heinz et al., 1993). Consequently, sequences flanking both VLI and VLI were incorporated into the bacterial architecture (Figure 2).

A glycine−alanine loop (GAL) mutant was constructed to ascertain the significance of the length of the VLI substitution. Glycines and alanines were incorporated in place of all vertebrate residues present in the VLI sequence, except the strictly conserved residues Leu-67 and Arg-70 (vertebrate numbering, Figure 2). In this case, productive interactions between these two residues and the folate substrate may be preserved if the GAL acts as an effective "spacer" between α-helix C and β-strand C.

Circular Dichroism Spectroscopy. Circular dichorism (CD) spectra were recorded for VLI and VLII DHFRs in an effort to assess the impact of the inserted vertebrate sequences on the structural integrity of the bacterial enzyme. Spectra were collected for mutant and wild-type *E. coli* DHFRs as described in the Materials and Methods section. The data collected for the wild-type enzyme are in agreement with previously published data (Greenfield et al., 1972; Greenfield, 1975). Spectra for wild-type, VLI, and VLII DHFRs are shown in Figure 3. It is apparent that the insertions have had an effect on the global conformation of VLII but not VLI relative to the wild-type DHFR.

Steady-State Kinetics. The steady-state parameters k_{cat} and K_m were determined for mutant DHFRs by holding the concentration of NADPH constant (100 μM) and varying the concentration of H_2F or by holding the concentration of H_2F constant (30 μM) and varying the concentration of NADPH (Stone & Morrison, 1982; Fierke et al., 1987). For all of the mutant enzymes, double-reciprocal plots were linear over all concentrations of coenzyme and substrate (data not shown).

The pH dependencies of k_{cat} and k_{cat}/K_m were determined for all mutant DHFRs. The maximum values (pH independent) of these parameters are listed in Table 1. For the VLI and VLII mutants, the maximum values of k_{cat} and K_m are relatively unchanged with respect to the wild-type bacterial enzyme; however, the pH dependencies of these parameters differ significantly (Figure 4a,b). In the case of the VLII mutant, a pH dependence is observed in K_m for H_2F at pH's greater than 7.0 (Figure 4b). As a result, the pK_a observed for k_{cat}/K_m is shifted approximately 0.6 unit below that of wild-type *E. coli* DHFR (7.5 vs 8.1). On the other hand, the pK_a value for k_{cat} is shifted 0.5 unit higher than the bacterial enzyme.

Differences between the VLI mutant and the bacterial enzyme are confined primarily to the pK_a's associated with k_{cat} and k_{cat}/K_m. Qualitatively, both profiles appear to describe three pK_a's (Figure 4a); however, pre-steady-state and transient binding studies suggest that the data can be fit to a two-pK_a model, as described by eqs 5 and 6 (vide infra).

$$k_{cat} = \frac{B + B'([H]/K_b)}{[1 + ([H]/K_b)][1 + (K_a/[H])]} \quad (5)$$

In eq 5, B is the maximum value of k_{cat} over the entire pH range, and B' is the value of k_{cat} at pH < 5.0. K_a and K_b are the apparent acid and base dissociation constants, respectively. With the exception of B', values for these parameters are displayed in Table 1, with the parameter B representing the maximum value of k_{cat}. The parameter B' was determined to be 3.0 ± 0.4 s^{-1}. In the absence of a measurable pH dependence in the K_m for H_2F, k_{cat}/K_m follows the same dependence on pH as k_{cat}.

In eq 6, C' is the plateau value of k_{cat}/K_m at low pH, and C is the maximum value of this parameter. The following

$$k_{cat}/K_m = \frac{C + C'([H]/K_b)}{[1 + ([H]/K_b)][1 + (K_a/[H])]} \quad (6)$$

parameters were determined by fitting the data to eq 6: C = 11 ± 1 μM^{-1} s^{-1}, C' = 3 ± 0.5 μM^{-1} s^{-1}, pK_a = 8.7 ± 0.1, and pK_b = 6.9 ± 0.3. The pK_a's determined here are apparent values and are a function of pH dependencies in hydride transfer (pK_1) and product release (pK_2; see Discussion).

For the GAL mutant, the K_m for H_2F and the pK_a's for k_{cat} and k_{cat}/K_m are dramatically different from those of the wild-type *E. coli* enzyme. The K_m for H_2F is increased by roughly 55-fold, and the pK_a's for k_{cat}/K_m and k_{cat} are shifted approximately 0.9 and 1.7 units lower, respectively (Table 1).

All of the loop mutants were assayed for enhanced specificity for folic acid reduction at pH 6, and those results are presented in Table 2. VLI DHFR exhibited a 13-fold increase in specificity for folate, which can be mainly

Table 1: Steady-State Parameters for Chicken and *E. coli* Reductases

	dihydrofolate reductase				
parameter	*E. coli*[a]	VLI	GAL	VLII	avian
k_{cat} (s^{-1})	12.3	11.2 ± 1.1	16.0 ± 2.0	4.5 ± 0.5	9.8[b]
K_m (H_2F, μM)	0.7	1.0 ± 0.1	36.7 ± 0.5	1.4 ± 0.2	0.12[b]
pK_a (k_{cat})	8.4	8.7 ± 0.1	6.7 ± 0.2	8.9 ± 0.1	8.6[b]
pK_b (k_{cat})		6.9 ± 0.1			
k_{cat}/K_m (μM^{-1} s^{-1})	18	11 ± 2	0.44 ± 0.08	3.9 ± 0.6	80[b]
pK_a (k_{cat}/K_m)	8.1	8.7 ± 0.1	7.2 ± 0.1	7.5 ± 0.1	7.9[b]
pK_b (k_{cat}/K_m)		6.9 ± 0.3			
$^HV/^DV$	1.0 (pH 6.0)	0.9 ± 0.1 (pH 6.0)	2.9 ± 0.2 (pH 6.0)	1.2 ± 0.1 (pH 6.3)	1.0 ± 0.1 (pH 6.0)
$^HV/^DV$	3.2 (pH 10.0)	2.5 ± 0.1 (pH 9.0)		2.8 ± 0.1 (pH 9.8)	2.5 ± 0.1 (pH 9.0)

[a] Fierke et al. (1987) and references therein. [b] Morrison and Stone (1986).

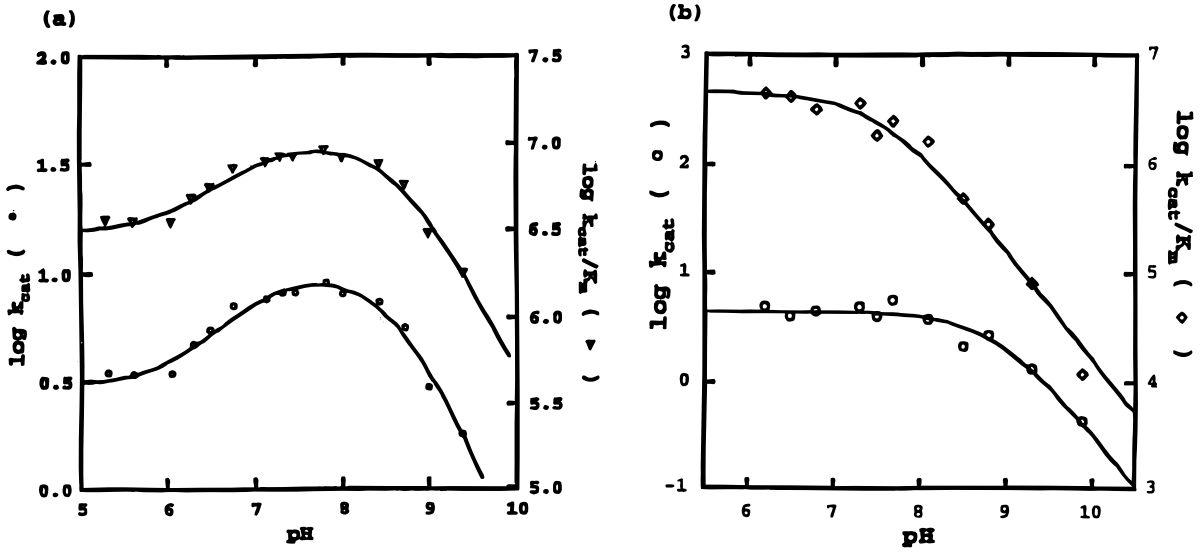

FIGURE 4: pH dependencies of k_{cat} and K_m for VLI DHFR (a) and VLII DHFR (b). The relationship of the apparent pK_a's (pK_a and pK_b) observed for VLI DHFR is considered in detail in the Discussion section, with references to Figures 6 and 7 (see text).

Table 2: Folate Reduction by *E. coli* and Chicken DHFRs at pH 6.0

	dihydrofolate reductase				
parameter	*E. coli*	VLI	VLII[a]	GAL	avian[b]
$k_{cat} \times 10^3$ (s^{-1})	3.7 ± 0.2	4.6 ± 0.2	<1.0	<1.0	160
K_m (μM)	9.4 ± 1.5	0.9 ± 0.2	ND	ND	1.1
$V/K \times 10^2$ (M^{-1} s^{-1})	3.9 ± 0.6	51 ± 11	ND	ND	1500

[a] Not Determined. [b] Taken from Morrison and Stone (1986).

Table 3: Equilibrium Binding Constants at pH 6.0

	K_d (nM)				
ligand	*E. coli*[a]	VLI	GAL[b]	VLII	avian
H_2F	220	23 ± 2		393 ± 46	10 ± 1.4
folate	1000 ± 100	161 ± 6		1240 ± 140	140 ± 9
NADPH	330	153 ± 3	970 ± 30	3020 ± 260	36 ± 3
NADP	24000	21000 ± 140			

[a] Taken from Fierke et al. (1987). [b] Except for NADPH, fluorescence quenching by ligands was too small to permit the determination of thermodynamic dissociation constants.

accounted for by a 10-fold decrease in K_m. The VLII and GAL DHFRs did not reduce folate at a measurable rate. Consequently, we chose to characterize only the VLI and GAL DHFRs more extensively.

Thermodynamic Binding Constants. The binding of MTX, NADPH, NADP, folate, H_2F, and H_4F to DHFR is accompanied by a decrease in intrinsic protein fluorescence at 340 and 325 nm for bacterial and vertebrate reductases, respectively (Fierke et al., 1987; Taira & Benkovic, 1988; Appleman et al., 1990a; Thillet et al., 1990). Fluorescence titration curves were generated for several ligands bound to the various DHFRs, and the calculated thermodynamic dissociation constants are shown in Table 3.

Relaxation Experiments. The formation of binary complexes of DHFR with the coenzyme, H_2F, or folate results in a quenching of intrinsic protein fluorescence. Under pseudo-first-order conditions, two exponential decays are typically observed: a rapid, ligand-dependent phase and a slower, ligand-independent phase (Dunn et al., 1978; Dunn & King, 1980; Cayley et al., 1981). For binding of the coenzyme, a simple mechanism was suggested in which NADPH preferentially binds to one of two enzyme conformers (E_1) and interconversion between the conformers is slow (Scheme 1). The ratio of the amplitudes for the fast and slow phases is indicative of the E_1/E_2 equilibrium (K_{eq}).

Scheme 1

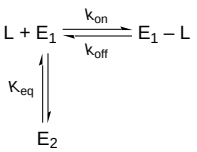

$K_{eq} = [E_1]/[E_2] = k_{iso}/k_{iso}'$

Over a wide range of concentrations (1−200 μM), binding of the coenzyme to VLI and GAL DHFRs could be described by this two-exponential model (Figure 5). The observed rate

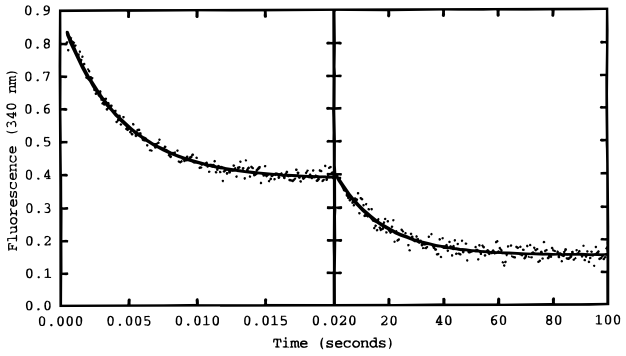

FIGURE 5: Binding of NADPH to VLI DHFR. Relaxation data were collected for VLI DHFR and NADPH over two time scales. Final conditions were as follows: 1.0 μM DHFR and 7.5 μM NADPH in MTEN, pH 6.0.

constant for the ligand-dependent phase was found to increase linearly with ligand concentration, without showing any signs of saturation (data not shown). The observed E_1/E_2 equilibrium (K_{eq}) was 2.1 ± 0.1 for the VLI mutant and 0.94 ± 0.1 for the GAL mutant. In both cases, the rate constant for the E_2 to E_1 conversion was similar to that of the wild-type *E. coli* enzyme (VLI, 0.059 ± 0.006 s^{-1}; GAL, 0.048 ± 0.005 s^{-1}; wild type, 0.032 ± 0.002 s^{-1}). Data for NADPH binding to VLI and GAL are presented in Table 4.

Similar experiments were carried out for the binding of H_2F and folate. Binding of either ligand to GAL could not be characterized due to low fluorescence quenching upon complex formation. For VLI DHFR, a rapid ligand-dependent phase and a slower ligand-independent phase were observed in relaxation experiments with H_2F and folate. Kinetic data for folate and H_2F binding are shown in Table 4 for wild-type *E. coli* and VLI DHFRs.

For the binding of H_2F, NADPH, and folate to the parent bacterial reductase, the equilibrium between unliganded conformers is 1.0 ($K_{eq} = E_1/E_2$, Scheme 1; Cayley et al., 1981; Fierke et al., 1987). In the case of the VLI mutant, the ratio of the amplitudes of the fast and slow phases for the binding of H_2F or folate (K_{eq}) was 9.8 ± 1.0, not the anticipated 2.2. The difference in conformer distribution observed between binding experiments with NADPH and the pterin substrates is not readily explained from these data. However, a similar observation has been made for the wild-type *E. coli* DHFR and a mutant of this enzyme (D27N) binding to NADPH and MTX (Appleman et al., 1988). For both enzymes, a significantly larger population of conformers rapidly bind to the latter ligand. Therefore, it should be borne in mind that while the designations "E_1" and "E_2" are useful in describing the kinetics of binding of a particular ligand, the conformations that they represent are ligand dependent and may not be the same.

Competition Experiments. Competition experiments measure the off rate (k_{-1}) of a particular ligand from a complex with DHFR (Scheme 2; Dunn et al., 1978; Birdsall et al., 1980). Dissociation rate constants determined for various binary and ternary complexes GAL and VLI by this method are displayed in Table 5. These data were generally in good agreement with those measured by relaxation; however, for values $k_{off} < 5$ s^{-1}, the competition method provides the more accurate values and these are incorporated in Table 4.

From these results, Scheme 1 is adequate to describe the binding of NADPH, H_2F, and folate to the mutant reductases. According to this mechanism, the K_d is given by eq 7 and should be predicted by the rate constants determined by relaxation and competition methods. The calculated thermodynamic dissociation constants are generally in good agreement with the observed K_d's for NADPH, H_2F, and folate binding to VLI and GAL DHFRs (Table 4).

$$K_d = (k_{off}/k_{on})(1 + 1/K_{eq}) \quad (7)$$

An important feature of the mechanism for wild-type *E. coli* DHFR is a dominant pathway for product release (Scheme 3). Following the hydride-transfer step, NADP rapidly dissociates from the product ternary complex to generate E−H_4F. Less than 1.3% of the enzyme forms E−NADP as a result of dissociation of H_4F from the product ternary complex. Subsequent binding of NADPH to E−H_4F accelerates the dissociation of H_4F by 9-fold compared to its dissociation from the binary complex. Thus, during the catalytic cycle, no free enzyme is generated. This binding antagonism between H_4F and NADPH also accelerates the dissociation of NADPH from the mixed ternary complex (E−NADPH−H_4F). The off rates of NADPH from the binary and mixed ternary complexes are 3.5 and 85 s^{-1}, respectively.

The off rates (Table 5) measured for VLI DHFR indicate that the same dominant pathway for product release is operative under steady-state conditions. Less than 2% of the enzyme is converted to E−NADP following hydride transfer. The remaining enzyme forms E−H_4F as a result of rapid dissociation of NADP from the product ternary complex (125 s^{-1}).

At pH 6.0, however, the binding antagonism between NADPH and H_4F is no longer reflected in the rate constants for the pertinent complexes. Although dissociation of NADPH from the mixed ternary complex is still rapid (110 s^{-1}), the off rates of H_4F from the binary and mixed ternary complexes are comparable (2.6 vs 3.5 s^{-1}). Measurement of the off rate of H_4F from E−NADPH−H_4F as a function of pH shows that it increases in a sigmoidal fashion from 3.5 s^{-1} at pH 5.0 to 27 s^{-1} at pH 9.0 (Figure 6). At pH's between 5.0 and 7.0, this off rate closely approximates the observed steady-state rate. Therefore, the E−NH−H_4F complex must be the species that accumulates in the steady state over this pH range.

We and others have interpreted this pH dependence to arise from a single ionization, as described by Scheme 4 (Li & Benkovic, 1991; Appleman et al., 1992). In a helix-exchange experiment, Li noted the possibility that Asp-27 is the ionizing residue on the basis of the observation that none of the new residues incorporated into *E. coli* DHFR could account for the observed pK_a. Although a new acidic residue is present in VLI DHFR (Figure 2), this residue (E52) should be near the surface of the protein and does not interact directly with bound folate (Davies et al., 1990). It has been suggested that the pH dependence may be due to a global ionization consisting of several residues (Appleman et al., 1992; Chen, et al., 1994).

The pH dependence of the off rate from Scheme 4 is given by eq 8, where k_{off}' and k_{off} are the rate constants for dissociation of H_4F from the ionized and un-ionized forms of E−NADPH−H_4F, respectively, and K_b is the ionization constant of a group on the enzyme. For VLI DHFR, k_{off}, k_{off}', and pK_b were determined to be 3.5 s^{-1}, 27 s^{-1}, and 7.5,

Table 4: Summary of Ligand Binding Experiments

DHFR	ligand	K_{eq}	k_{on} (μM^{-1} s^{-1})	k_{off} (s^{-1})	K_d (nM)	K_d (nM), predicted
wt	NADPH	1.0	20 (E_1) 5 (E_2)	3 70	330	297
VLI	NADPH	2.1 ± 0.1	29.5 ± 0.9	2.8 ± 0.2	153 ± 3	142
GAL	NADPH	0.9 ± 0.1	41 ± 5.7	47 ± 0.6	970 ± 30	2000
wt	H_2F	1.0	42	22	220	1000
VLI	H_2F	9.8 ± 1.0	20 ± 0.4	0.87 ± 0.07	23 ± 2	47
wt	folate	1.0	57 ± 5.0	35 ± 12	1000 ± 100	1230
VLI	folate	9.5 ± 1.0	19 ± 1.0	3.5 ± 0.2	161 ± 6	203

Scheme 2

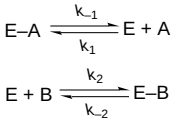

Table 5: Ligand Dissociation Rate Constants

ligand	enzyme species	trapping ligand	k_{off} (s^{-1})[a]		
			E. coli[b]	VLI	GAL
NADPH	E−NADPH	NADP	3.5	2.8 ± 0.2	47 ± 0.6
folate	E−folate	H_2F		3.5 ± 0.2	
H_2F	E−H_2F	folate	22	0.87 ± 0.07	
H_4F	E−H_4F	MTX	1.4	2.6 ± 0.3	86 ± 1
H_4F	E−NADPH−H_4F	MTX	12.0	3.5 ± 0.1	251 ± 9
H_4F	E−NADP−H_4F	MTX	1.7	2.5 ± 0.1	103 ± 4
NADP	E−NADP−H_4F	NADPH	200	125 ± 5	120 ± 1
NADPH	E−NADPH−H_4F	NADP	85	110 ± 13	

[a] MTEN, pH 6.0. [b] Taken from Fierke et al. (1987).

Scheme 3

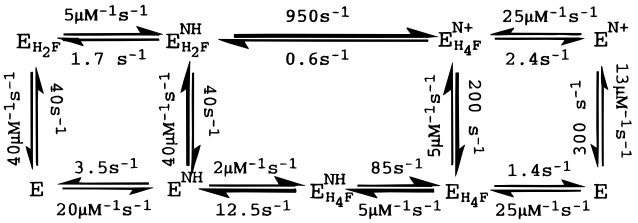

respectively.

$$k_{obs} = \frac{k_{off} + k_{off}'([H]/K_b)}{1 + ([H]/K_b)} \quad (8)$$

In contrast to the results with VLI DHFR, a dominant pathway for product release does not appear to be operative for the GAL mutant (Table 5). Approximately 50% of the enzyme is converted to E−NADP following hydride transfer, while the remainder loses NADP to generate E−H_4F. Moreover, NADPH increases the off rate of H_4F by only 3-fold compared to the off rate from the binary complex.

Pre-Steady-State Kinetics. Pre-steady-state experiments were conducted by observing the change in absorbance at 340 nm. For VLI DHFR, a burst of product formation is observed followed by a linear steady-state rate. By using a simple model of single-exponential decay followed by linear decay, the observed kinetic parameters were as follows for data collected at pH 7.0 and 25 °C: $k_{burst} = 152 \pm 10$ s^{-1}, $k_{ss} = 7.6 \pm 0.5$ s^{-1}, and $amp_{burst}/[E] = 0.7 \pm 0.1$ (data not shown). A full primary deuterium isotope effect of 3.2 ± 0.3 was observed when the experiment was repeated with [4′(*R*)-^{2}H]NADPH in place of NADPH. This confirmed that the burst is in fact due to hydride transfer. Data collected

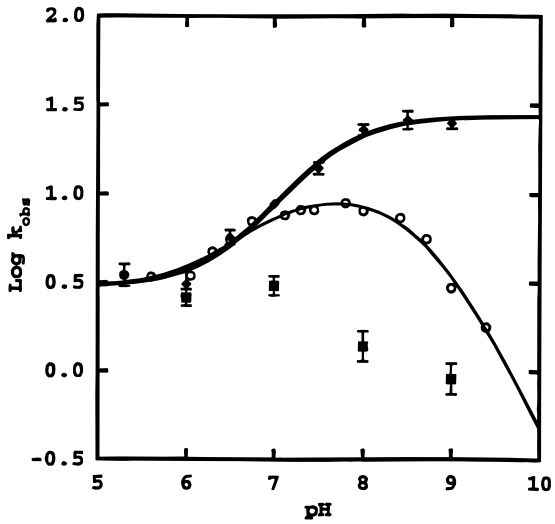

FIGURE 6: pH dependencies of the off rates of H_4F from E−NADPH−H_4F and E−H_4F for VLI DHFR. Data are shown as the logarithm of k_{obs} vs pH for E−H_4F (■) and E−NADPH−H_4F (◆). The pH dependence of k_{cat} (○) is determined by the off rate of H_4F from E−NADPH−H_4F.

Scheme 4

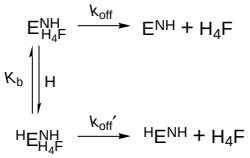

and analyzed on the stopped-flow computer were subsequently transferred to a Vax microcomputer, where the forward rate of hydride transfer was determined by using the simulation program KINSIM (Barshop et al., 1983) and Scheme 5. The rate constants used in these simulations were taken from Tables 4 and 5 (Fierke et al., 1987) and Scheme 4. The remaining rate constants, k_2, k_3, k_4, and k_{-hyd}, were assumed to be the same as the wild-type *E. coli* enzyme (Fierke et al., 1977). All are collected in the legend to Figure 7. Hydride-transfer rates then were estimated at several pH's (Figure 7). Fitting of the data to eq 2 yielded an intrinsic pK_a of 6.6 ± 0.1 for Asp-27 in the substrate ternary complex and a maximal hydride-transfer rate of 500 ± 43 s^{-1}.

Previous studies have attributed the pH dependence observed in hydride transfer to the ionization state of Asp-27, the only acidic residue in the folate binding pocket capable of donating a proton to N5 (Fierke et al., 1987). A recent study has proposed that the observed pK_a is due to the ionization of N5 of H_2F in the E−NADPH−H_2F complex (Chen et al., 1994). The authors argue that Asp-27 is ionized from pH 5 to 10 and serves as an "ion anchor" that stabilizes the surrounding water structure. The proton is presumably supplied by the ambient solution via a bound water molecule

Scheme 5

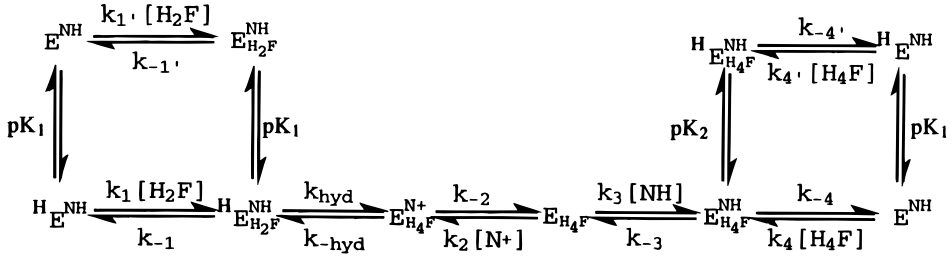

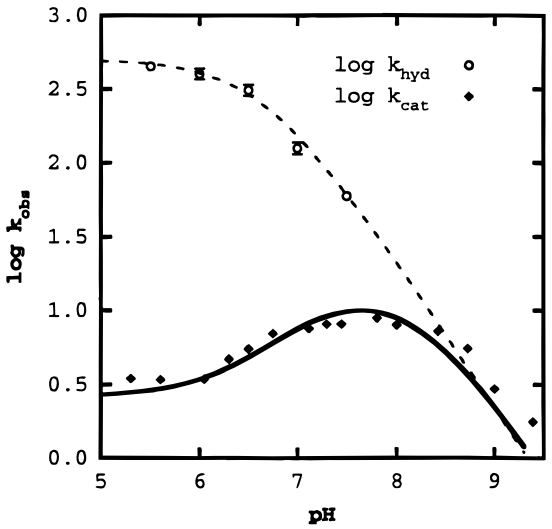

FIGURE 7: pH dependence of hydride transfer and simulation of steady-state turnover for VLI DHFR. Data are shown as the logarithms of k_{hyd} (○) and k_{cat} (◆) vs pH. The dashed line is the best fit for k_{hyd} as a function of pH using eq 2 (see text). The heavy solid line is the simulated pH dependence of k_{cat} using Scheme 5. The following rate constants were incorporated into simulations with Scheme 5 (varying $[H^+]$): $k_{hyd} = 500\ s^{-1}$, $k_{-hyd} = 0.06\ s^{-1}$, $k_2 = 5\ \mu M^{-1}\ s^{-1}$, $k_{-2} = 125\ s^{-1}$, $k_3 = 8.5\ \mu M^{-1}\ s^{-1}$, $k_{-3} = 110\ s^{-1}$, $k_4 = 2\ \mu M^{-1}\ s^{-1}$, $k_{-4} = 27\ s^{-1}$, $k_{4'} = 5\ \mu M^{-1}\ s^{-1}$, $k_{-4'} = 3.5\ s^{-1}$, $pK_1 = 6.6$, and $pK_2 = 7.5$. In all simulations, it was assumed that the pK_a's of the binary and ternary substrate complexes are the same, since a pH dependence was not detected in the K_m or K_d of H_2F (Fierke et al., 1987).

proximal to N5. The two rationales are kinetically indistinguishable. How the holoenzyme raises the pK_a of N5 from its solution value of 2.6 to 6.5 on the enzyme is not clear.

The rate constants determined by transient binding and pre-steady-state kinetics should predict steady-state turnover at any ligand concentration or pH (Fierke et al., 1987). In the case of VLI, values for k_{cat} were determined at several pH's by using Scheme 5 (Figure 7). Discrepancies between simulated and observed values of k_{cat} at high pH are probably a result of the difficulty in determining the pK_a governing the hydride-transfer step. Due to poor signal to noise ratios, data were not obtained at pH > 7.5.

A burst of product formation was not observed for GAL DHFR under pre-steady-state conditions. The observed rate was pH dependent, and analysis of the data by using eq 2 yielded a maximum rate of hydride transfer of $24 \pm 2\ s^{-1}$ and an intrinsic pK_a of 6.4 ± 0.1 (data not shown). A primary deuterium isotope effect of 3.0 ± 0.3 was observed in experiments conducted with NADPH and repeated with [4′(*R*)-^{2}H]NADPH. These results confirm conclusions made on the basis of steady-state data and primary deuterium isotope effects on k_{cat}. In particular, hydride transfer is rate limiting for steady-state turnover at all pH's, and the pK_a observed for k_{cat} is in fact the intrinsic pK_a of the E-NADPH−H_2F complex.

DISCUSSION

Preliminary Characterization of Mutant and Wild-Type DHFRs. The VLII mutation results in a mildly impaired reductase that has an apoenzyme structure that significantly differs from that of the parent enzyme (Figure 3). However, preincubation with substrate or coenzyme appears to induce a catalytically competent complex. A small primary deuterium isotope effect at low pH suggests that hydride transfer is still rapid and only partially rate limiting for steady-state turnover. Despite perturbations in NADPH binding (Table 3), no evidence was obtained for branched pathways for product release and/or substrate binding (Adams et al., 1989; Appleman et al., 1990b). Collectively, these observations suggest that the pathway for turnover is the same as that for the parent enzyme (Scheme 3). Given the location of the mutation (Figure 1) and the extent of the modifications to the bacterial architecture (seven inserted residues and four flanking substitutions), the kinetic and thermodynamic properties of this mutant are remarkable.

Nevertheless, the structure of the apoenzyme is significantly different from that of the wild-type *E. coli* reductase (Figure 3). This, in conjunction with the prolonged kinetic hysteresis and its inability to reduce folate, precluded in-depth kinetic analysis. One may conjecture as to how a loop of this size might be accommodated by the bacterial architecture. Medium-sized loops (6−10 residues in length) can be stabilized by packing of a residue on the loop into the protein, hydrogen bonding of inward-pointing main chain polar groups, and/or contacts with other elements of secondary structure on the protein surface (Tramontano et al., 1989). Alternatively, the inserted residues may have dictated new boundaries for secondary structure throughout this region of the protein, and, consequently, the vertebrate *sequence* does not necessarily exist as the vertebrate *substructure* in the mutant reductase. The latter possibility has been illustrated in mutagenesis studies of staphylococcal nuclease and bacteriophage T4 lysozyme (Sondek & Shortle, 1990; Sondek & Shortle, 1992; Heinz et al., 1993).

Crystallographic data for chicken and human DHFRs and the dynamic data described here leads us to favor the former possibility. The crystal structure for the chicken reductase reveals that VLII makes contact with another loop that connects α-helix E and β-strand E (residues 100−110, Figure 1). It has been suggested that this contact stabilizes VLII (Volz et al., 1982). Given the large size of this substructure compared to bacterial loop II, contacts between VLII and other parts of the bacterial enzyme are probable. It has been argued that this region of the protein should have a nominal effect on the flexibility of the molecule and catalytic

efficiency (Bystroff & Kraut, 1991). Clearly, this cannot be the case for the apoenzyme form of the mutant, as evidenced by its circular dichroism spectrum (Figure 3) and hysteretic behavior. The apoenzyme structure is different from, and catalytically less efficient than, the corresponding structure of the wild-type bacterial DHFR. However, active site titration of the holoenzyme with MTX demonstrated that ≥90% of the protein is active. The apoprotein may be in a stable, but partially unfolded conformation. On the basis of the relatively small perturbations in the K_d's and the kinetics of the holoenzyme (E−NADPH), a multiplicity of favorable enzyme−ligand interactions may dictate a catalytically competent and conceivably wild-type-like structure. Structural studies of the apo- and holoenzyme structures of the mutant should prove enlightening on this point.

In contrast, the results obtained with the VLI mutant are promising relative to the objective of conferring folate specificity. The effect of the mutation has not produced severe global alterations in the bacterial structure (Figure 3). The effects of the mutation are localized to the pterin binding site and have produced a reductase with hybrid properties. The affinity of the mutant enzyme for folate and H_2F is comparable to that of the chicken enzyme (Table 3). Enhanced specificity for folate relative to the *E. coli* enzyme is observed that is a consequence of increased affinity of the mutant E−NADPH complex for folate (Table 2). To date, this is the only mutation of *E. coli* DHFR to result in an increase in affinity and specificity for folate.

The GAL mutant was designed to test the validity of our considerations in the design of VLI DHFR. In essence, we assumed that the sequence integrity of the loop conformation is unimportant in allowing conserved residues (Leu-54 and Arg-57, *E. coli* numbering in Figure 2) to interact productively with the substrate. As evidenced by both the thermodynamic and kinetic data, the sequence within the loop conformation is vital for binding and catalysis. A large primary deuterium isotope effect with [4′(*R*)-^{2}H]NADPH demonstrates that steady-state turnover is limited by hydride transfer at all pH's. The inability to measure an equilibrium dissociation constant for H_2F, however, suggests a reorganization of the pterin binding site. However, a large conformational change was not indicated in its CD spectrum when compared with that of the wild-type enzyme (data not shown).

Binding and Catalysis by GAL and VLI DHFRs. The effect of both mutations is primarily localized to the pterin binding site. In binary complexes, the binding energy of VLI DHFR for H_2F and folate is increased by 1.3 and 1.0 kcal/mol, respectively. For VLI DHFR, the increased affinity is primarily due to large decreases (>25-fold) in the off rate of both substrates and also due in part to a 5-fold decrease in the population of low-affinity apoenzyme conformers (represented by E_2, Scheme 1). On the other hand, the K_m for H_2F binding to GAL DHFR is less favorable by 3.0 kcal/mol. By assuming that the K_m is equal to the K_d and the association rate constant is unchanged (40 μM^{-1} s^{-1}), the calculated off rate would be 740 s^{-1}, a value 34 times larger than the off rate of the wild-type reductase.

Binding of H_4F to product examples and mixed ternary complexes is affected in a similar fashion. Off rates of H_4F from E−NADPH−H_4F, E−NADP−H_4F, and E−H_4F are increased by 21-, 41-, and 61-fold, respectively, for GAL DHFR compared to the parent reductase. With the loss of binding antagonism between NADPH and H_4F, a dominant pathway for substrate binding and product release no longer dictates steady-state turnover. For VLI DHFR and wild-type enzyme, a pathway involving NADPH-mediated H_4F release is prominant below pH 7. The binding of H_4F to E, however, appears to improve with increasing pH, while the opposite trend prevails for the binding of H_4F to E−NADPH. The latter pH dependency results in dissociation rates from E−H_4F and E−NADPH−H_4F that are coincident with steady-state turnover at pH's between 5 and 7. In general, there is close quantitative correspondence between these rate constants and those for the wild-type enzyme.

At least two explanations may account for the unusual pH dependence in this dissociation rate observed for the VLI mutant. After hydride transfer, H_4F may equilibrate to a conformation on the enzyme where direct interaction with the coenzyme is minimized. X-ray crystallographic studies of the wild-type *E. coli* reductase have postulated that binding cooperativity observed for coenzyme and substrates, products, and inhibitors is largely determined by the degree of overlap between the two binding sites (Bystroff & Kraut, 1991). For example, the major difference in the binding geometries of the inhibitor MTX and H_2F in ternary complexes with NADPH is a 180° rotation of the pterin ring about an axis of rotation passing through the C6−C9 bond (Bolin et al., 1982; Bystroff et al., 1990). It has also been inferred that the close contact of the nicotinamide and pterin rings in the mixed ternary complex also accounts for the negative cooperativity observed for NADPH and H_4F (Bystroff & Kraut, 1991; Reyes et al., 1995). In the case of VLI DHFR, it is plausible that H_4F equilibrates to a binding geometry approximating that of MTX prior to dissociation from the enzyme and that protonation is important for mediating this conformational change. This argument is summarized in Scheme 5, where the individually measured rate constants predict different intrinsic pK_a's for the substrate ternary complex and the mixed product ternary complex (E−NH−H_4F).

Secondly, it has also been suggested that several distal ionizations cause structural perturbations that in turn alter affinity for H_4F in the mixed ternary complex (Appleman et al., 1992). The fact that the off rate for NADPH from the E−NADPH−H_4F complex is largely unaffected in the VLI mutant suggests that ligand cooperativity is probably more complex than structural studies have indicated. Given the feasibility of structural characterization of H_4F analogues bound to *E. coli* DHFR (Reyes et al., 1995), it should be possible to determine the interactions that dictate the kinetics of H_4F dissociation.

The effects of the GAL mutation on binding and catalysis are surprisingly similar to those described for a series of point mutations at Leu-54 [Table 6; Murphy & Benkovic, 1989). Leu-54 is a strictly conserved residue in bacterial and vertebrate DHFRs that occurs in the loop between α-helix C and β-strand C where the glycine and alanine substitutions and insertions were made to construct GAL DHFR (*E. coli* numbering, Figure 2). When Leu-54 is mutated to isoleucine, asparagine, or glycine, the K_m constants for H_2F increase in the order of Leu < Ile < Asn < Gly. For the mutants, the extremes are represented by the isoleucine and glycine substitutions, which result in 10- and 1700-fold increases in K_d or K_m, respectively (Table 6). Unexpectedly, the activation energy for hydride transfer was increased by ap-

Table 6: Selected Kinetic Parameters for Mutant and Wild-Type *E. coli* DHFRs for the Reduction of Dihydrofolate

		H_2F				
DHFR	NADPH K_d (μM)	K_d (μM)	K_m (μM)	k_{cat} (s^{-1})	k_{cat}/K_m (μM^{-1} s^{-1})	k_{hyd} (s^{-1})
wt[a]	0.330	0.220	0.7	12.0	18.0	950
D27E[b]			27	41.0	1.50	460
L54I[c]	0.300	1.90	26	31	1.20	31
L54N[c]	0.590		75	42	0.560	42
L54G[c]	0.020		350	29	0.083	29
GAL	0.970		37	16.0	0.440	24
VLI	0.153	0.025	1.0	11.0	11.0	500
D27E/VLI[d]			1.3	18.0	14.0	
D27E/L28V/VLI[d]			5.6	12.0	2.14	

[a] Fierke et al. (1987). [b] David et al. (1992). [c] Murphy and Benkovic (1989). [d] Posner and Benkovic, unpublished.

proximately 2.0 kcal/mol for all mutations at this position. As a result, the chemical step is rate limiting for steady-state turnover at all pH's. The GAL mutation effectively replaces all of the polar residues in the VLI sequence with hydrophobic residues, except Arg-60 (VLI numbering, Figure 2). One would expect substantial repacking of this otherwise solvent-exposed region, with rather dramatic consequences for binding and catalysis. However, GAL DHFR binds H_2F better than the L54G and L54N mutants and catalyzes hydride transfer at a rate comparable to all of the point mutations at this position (Table 6). In addition, the binding of NADPH is only mildly weakened, the equilibrium between apoenzyme conformers is still 1.0, and the intrinsic pK_a of the E−NADPH−H_2F complex is unaltered. Clearly, the structural transition between ground-state binding and transition-state stabilization is complicated. Yet in terms of binding and catalysis, the global structure of the enzyme appears to limit the effects of all mutations within this region to 2−3 kcal/mol.

In the context of VLI DHFR, the roles of Leu-54 and Arg-57 appear to be remarkably preserved. The activation energy for hydride transfer was increased by only 0.4 kcal/mol, and the dynamics of product release and substrate binding are only mildly perturbed. In addition, the binding of H_2F to E−NADPH is improved by roughly 10-fold (assuming $K_m = K_d$).

Folate Reduction. On the basis of these results, we considered two additional mutants of the VLI DHFR gene on the basis of available structural and kinetic data of the enzyme from avian or murine sources. These proteins feature glutamate and phenylalanine substitutions at positions −27 and −28 for key active site residues involved in the protonation of the pterin ring and its positioning relative to NADPH in the avian enzyme. Neither D27E/VLI nor D27E/L28F/VLI DHFR catalyzed the reduction of folate as well as wild-type *E. coli* DHFR (data not shown), and in both cases, specificity for H_2F was affected. It is interesting to note that specificity for H_2F was largely preserved in D27E/VLI DHFR as compared to the D27E mutation alone (Table 6). The VLI mutation appears to alter the active site dimensions to accommodate the role of the larger acidic residue in ground-state binding and most likely hydride transfer.

In view of the results obtained from VLI DHFR and its derivatives, it seems likely that several nonconserved features of the bacterial and vertebrate structures determine the differential specificity displayed by three reductases for folate. Perhaps the inability of the bacterial enzyme to protonate N8 of folate is repsonsible for the difference in specificity observed for *E. coli* and chicken DHFRs (Reyes et al., 1995). It may be necessary to incorporate several combinations of the nonconserved regions of the vertebrate reductase into the bacterial architecture to alter substrate specificity (Figure 1). In addition to loop and turn substructures, helix exchange may be required as well (Li & Benkovic, 1991). Of course, the exchange of structural elements is certainly complicated by determining how much of the vertebrate substrate to incorporate into the bacterial enzyme such that structural initiation and termination motifs are preserved. Given the complexity of the problem and the labor involved in constructing and characterizing each mutant, a screening or selection strategy must be developed to facilitate characterization (Howell et al., 1986; Hermes et al., 1987; Fetrow et al., 1989; Oliphant & Struhl, 1989; McCafferty et al., 1990; Barbas et al., 1991; Kang et al., 1991; Poole et al., 1991; Hoogenboom et al., 1992).

ACKNOWLEDGMENT

We thank Jean Huang, Carston Wagner, Particia Jennings, Craig Mann, and Robert Matthews for many insightful discussions. We are grateful to Robert Matthews for allowing us to use his spectropolarimeter and to Patricia Jennings and Craig Mann for technical assistance. We thank Jean Huang for providing wild-type *E. coli* DHFR. We are indebted to John Morrison for communicating the purification procedure for chicken liver dihydrofolate reductase and to Kaye Yarnell for her patience and skill in preparing the manuscript.

REFERENCES

Adams, J., Johnson, K., Matthews, R., & Benkovic, S. J. (1989) *Biochemistry 28*, 6611−6618.
Andrews, J., Fierke, C. A., Birdsall, B., Ostler, G., Feeney, J., Roberts, G. C. K., & Benkovic, S. J. (1989) *Biochemistry 28*, 5743−5750.
Appleman, J. R., Howell, E. E., Kraut, J., Kuhl, M., & Blakley, R. (1988) *J. Biol. Chem. 263*, 9187−9198.
Appleman, J. R., Beard, W. A., Tavner, T. J., Prendergast, N. J., Freisheim, J. H., & Blakley, R. L. (1990a) *J. Biol. Chem. 265*, 2740−2748.
Appleman, J. R., Howell, E. E., Kraut, J., & Blakley, R. L. (1990b) *J. Biol. Chem. 265*, 5579−5584.
Appleman, J. R., Tsay, J.-T., Freisheim, J. H., & Blakley, R. L. (1992) *Biochemistry 31*, 3709−3715.
Baccanari, D., Averett, P. D., Briggs, C., & Burchall, J. (1977) *Biochemistry 16*, 3566−3572.
Barbas, C. F., Kang, A. S., Lerner, R. A., & Benkovic, S. J. (1991) *Proc. Natl. Acad. Sci. U.S.A. 88*, 7978−7982.
Barshop, B. A. R., Wrenn, F., & Freiden, C. (1983) *Anal. Biochem. 130*, 134−145.
Birdsall, B., Burgen, A. S. V., & Roberts, G. C. K. (1980) *Biochemistry 19*, 3723−3731.
Blakley, R. L. (1960) *Nature (London) 188*, 231−232.
Blakley, R. L. (1985) in *Folates and Pterins* (Blakley, R. L., & Benkovic, S. J., Eds.) pp 191−253, Wiley and Sons, Inc., New York.
Bolin, J. T., Filman, D. J., Matthews, D. A., Hamlin, R. C., & Kraut, J. (1982) *J. Biol. Chem. 257*, 13650−13662.
Bystroff, C., & Kraut, J. (1991) *Biochemistry 30*, 2227−2239.
Bystroff, C., Oatley, S. J., & Kraut, J. (1990) *Biochemistry 29*, 3263−3277.
Cayley, P. J., Dunn, S. M. J., & King, R. W. (1981) *Biochemistry 20*, 874−879.
Cleland, W. W. (1977) *Adv. Enzymol. 45*, 273−387.

Curthoys, H. P., Scott, J. M., & Rabinowitz, J. C. (1972) *J. Biol. Chem. 247*, 1959−1964.
David, C. L., Howell, E. E., Farnum, M. F., Villafranca, J. E., Oatley, S. J., & Kraut, J. (1992) *Biochemistry 31*, 9813−9822.
Davies, J. F., Delcamp, T. J., Prendergast, N. J., Ashford, V. A., Freisheim, J. H., & Kraut, J. (1990) *Biochemistry 29*, 9467−9479.
Dunn, S. M. J., & King, R. W. (1980) *Biochemistry 19*, 766−773.
Dunn, S. M. J., Batchelor, J. G., & King, R. W. (1978) *Biochemistry 17*, 2356−2364.
Dunn, C. R., Wilks, H. M., Halsall, D. J., Atkinson, T., Clarke, A. R., Muirhead, H., & Holbrook, J. J. (1991) *Philos. Trans. R. Soc. London B 332*, 177−184.
Fairman, R., Shoemaker, K. R., York, E. J., Stewart, J. M., & Baldwin, R. L. (1989) *Proteins: Struct., Funct., Genet. 5*, 1−7.
Fersht, A., & Winter, G. (1992) *Trends Biochem. Sci. 17*, 292−294.
Fetrow, J. S., Cardillo, T. S., & Sherman, F. (1989) *Proteins: Struct., Funct., Genet. 6*, 372−381.
Fierke, C. A., Johnson, K. J., & Benkovic, S. J. (1987) *Biochemistry 26*, 4085−4092.
Greenfield, N. J. (1975) *Biochim. Biophys. Acta 403*, 32−46.
Greenfield, N. J., Williams, M. N., Poe, M., & Hoogsteen, K. (1972) *Biochemistry 11*, 4706−4711.
Harper, E. T., & Rose, G. D. (1993) *Biochemistry 32*, 7605−7609.
Hedstrom, L., Szilagyi, L., & Rutter, W. J. (1992) *Science 255*, 1249−1253.
Heinz, D. W., Baase, W. A., Dahlquist, F. W., & Matthews, B. W. (1993) *Nature (London) 361*, 561−564.
Hermes, J. D., Blacklow, S. C., & Knowles, J. R. (1987) *Cold Spring Harbor Symp. Quant. Biol. 52*, 597−602.
Hoogenboom, H. R., Marks, J. D., Griffiths, A. D., & Winter, G. (1992) *Immunol. Rev. 130*, 41−68.
Howell, E. E., Villafranca, J. E., Warren, M. S., Oatley, S. J., & Kraut, J. (1986) *Science 231*, 1123−1128.
Johnson, K. A., & Benkoic, S. J. (1990) in *The Enzymes* (Sigman, D. S., & Boyer, P. D., Eds.) pp 159−211, Academic Press, Inc., San Diego, CA.
Kang, A. S., Jones, T. M., & Burton, D. R. (1991) *Proc. Natl. Acad. Sci. U.S.A. 88*, 11120−11123.
Kaufman, B. T., & Kemerer, V. F. (1977) *Arch. Biochem. Biophys. 179*, 420−431.
Li, L., & Benkovic, S. J. (1991) *Biochemistry 30*, 1470−1478.
Matthews, D. A., Bolin, J. T., Burridge, J. M., Filman, D. J., Volz, K. W., & Kraut, J. (1985) *J. Biol. Chem. 260*, 392−399.
McCafferty, J., Griffiths, A. D., Winter, G., & Chiswell, D. J. (1990) *Nature (London) 348*, 552−554.
Murphy, D. J., & Benkovic, S. J. (1989) *Biochemistry 28*, 3025−3031.
Oliphant, A. R., & Struhl, K. (1989) *Proc. Natl. Acad. Sci. U.S.A. 86*, 9094−9098.
Penner, M. H., & Frieden, C. (1985) *J. Biol. Chem. 260*, 5366−5369.
Poole, L. B., Loveys, D. A., Hale, S. P., Gerlt, J. A., Stanczyk, S. M., & Bolton, P. H. (1991) *Biochemistry 30*, 3621−3627.
Presta, L. G., & Rose, G. D. (1988) *Science 240*, 1632−1641.
Reyes, V. M., Sawaya, M. R., Brown, K. A., & Kraut, J. (1995) *Biochemistry 34*, 2710−2723.
Richardson, J. S., & Richardson, D. C. (1988) *Science 240*, 1648−1652.
Sambrook, J., Fritsch, E. F., & Maniatis, T. (1989) *Molecular Cloning: A Laboratory Manual*, Cold Spring Harbor Laboratory Press, Cold Spring Harbor, NY.
Schmid, F. (1990) in *Protein Structure: A Practical Approach* (Creighton, T. E., Ed.) pp 251−285, IRL Press, Oxford, UK.
Sondek, J., & Shortle, D. (1990) *Proteins: Struct., Funct., Genet. 5*, 299−305.
Sondek, J., & Shortle, D. (1992) *Proteins: Struct., Funct., Genet. 13*, 132−140.
Stone, S. R., & Morrison, J. F. (1982) *Biochemistry 21*, 3757−3765.
Stone, S. R., & Morrison, J. F. (1983) *Biochim. Biophys. Acta 745*, 247.
Stone, S. R., & Morrison, J. F. (1986) *Biochim. Biophys. Acta 869*, 275−285.
Taira, K., & Benkovic, S. J. (1988) *J. Med. Chem. 31*, 129−137.
Taira, K., Chen, J.-T., Fierke, C. A., & Benkovic, S. J. (1987) *Bull. Chem. Soc. Jpn. 60*, 3025−3030.
Thillet, J., Adams, J. A., & Benkovic, S. J. (1990) *Biochemistry 29*, 5195−5202.
Tramontano, A., Chothia, C., & Lesk, A. M. (1989) *Proteins: Struct., Funct., Genet. 6*, 382−394.
Viola, R. E., Cook, P. F., & Cleland, W. W. (1979) *Anal. Biochem. 96*, 334−340.
Volz, K. W., Matthews, D. A., Alden, R. A., Freer, S. T., Hansch, C., Kaufman, B. T., & Kraut, J. (1982) *J. Biol. Chem. 257*, 2528−2536.
Wagner, C. R., Thillet, J., & Benkovic, S. (1992) *Biochemistry 31*, 7834−7840.
Wilks, H. M., Moreton, K. M., Halsall, D. J., Hart, K. W., Sessions, R. D., Clarke, A. R., & Holbrook, J. J. (1992) *Biochemistry 31*, 7802−7806.
Wu, Y.-D., & Houk, K. N. (1987) *J. Am. Chem. Soc. 109*, 2226−2227.
Wu, Y.-D., & Houk, K. N. (1991) *J. Am. Chem. Soc. 113*, 2353−2358.

BI9518095